Optimization of bull's eye structures for transmission enhancement

O. Mahboub[1], S. Carretero Palacios[2], C. Genet[1], F. J. Garcia-Vidal[3], Sergio G. Rodrigo[2], L. Martin-Moreno[2,4,*] and T. W. Ebbesen[1,*]

[1]*ISIS, University of Strasbourg and CNRS, UMR 7006, 8 allée G. Monge, 67000 Strasbourg, France*
[2]*Instituto de Ciencia de Materiales de Aragón and Departamento de Física de la Materia Condensada, CSIC-Universidad de Zaragoza, E-50009, Zaragoza, Spain*
[3]*Departamento de Física Teórica de la Materia Condensada, Universidad Autónoma de Madrid, E-28049 Madrid, Spain*
[4]*lmm@unizar.es*
[*]*ebbesen@isis-ulp.org,*

Abstract: We present an exhaustive exploration of the parameter space defining the optical properties of a bull's eye structure, both experimentally and theoretically. By studying the resonance intensity variations associated with the different geometrical features, several parameters are seen to be interlinked and scale laws emerge. From the results it is possible to give a simple recipe to design a bull's eye structure with optimal transmission properties.

©2010 Optical Society of America

OCIS codes: (050.1220) Apertures; (240.6680) Surface plasmons; (050.2770) Gratings; (050.1960) Diffraction theory; (050.6624) Subwavelength structures.

References and links

1. W. L. Barnes, A. Dereux, and T. W. Ebbesen, "Surface plasmon subwavelength optics," Nature **424**(6950), 824–830 (2003).
2. A. V. Zayats, I. I. Smolyaninov, and A. A. Maradudin, "Nano-optics of surface plasmon polaritons," Phys. Rep. **408**(3-4), 131–314 (2005).
3. T. W. Ebbesen, C. Genet, and S. I. Bozhevolnyi, "Surface-plasmon circuitry," Phys. Today **61**(5), 44–50 (2008).
4. C. Genet, and T. W. Ebbesen, "Light in tiny holes," Nature **445**(7123), 39–46 (2007).
5. T. Thio, K. M. Pellerin, R. A. Linke, H. J. Lezec, and T. W. Ebbesen, "Enhanced light transmission through a single subwavelength aperture," Opt. Lett. **26**(24), 1972–1974 (2001).
6. T. Thio, H. J. Lezec, T. W. Ebbesen, K. M. Pellerin, G. D. Lewen, A. Nahata, and R. A. Linke, "Giant optical transmission of sub-wavelength apertures: physics and applications," Nanotechnology **13**(3), 429–432 (2002).
7. H. J. Lezec, A. Degiron, E. Devaux, R. A. Linke, L. Martin-Moreno, F. J. Garcia-Vidal, and T. W. Ebbesen, "Beaming light from a subwavelength aperture," Science **297**(5582), 820–822 (2002).
8. A. Nahata, R. A. Linke, T. Ishi, and K. Ohashi, "Enhanced nonlinear optical conversion from a periodically nanostructured metal film," Opt. Lett. **28**(6), 423–425 (2003).
9. L. Martín-Moreno, F. J. García-Vidal, H. J. Lezec, A. Degiron, and T. W. Ebbesen, "Theory of highly directional emission from a single subwavelength aperture surrounded by surface corrugations," Phys. Rev. Lett. **90**(16), 167401 (2003).
10. F. J. Garcia-Vidal and L. Martin-Moreno, H. J. Lezec and T. W. Ebbesen, "Focusing light with a single subwavelength aperture flanked by surface corrugations," Appl. Phys. Lett. **83**, 4500 (2003).
11. A. Degiron, and T. W. Ebbesen, "Analysis of the transmission process through single apertures surrounded by periodic corrugations," Opt. Express **12**(16), 3694–3700 (2004).
12. T. Ishi, J. Fujikata, K. Makita, T. Baba, and K. Ohashi, "Si Nano-Photodiode with a Surface Plasmon Antenna," Jpn. J. Appl. Phys. **44**(12), L364–L366 (2005).
13. S. Shimada, J. Hashijume, and F. Koyama, "Surface plasmon resonance on microaperture vertical-cavity surface-emitting laser with metal grating," Appl. Phys. Lett. **83**(5), 836–838 (2003).
14. B. Guo, G. Song, and L. Chen, "Plasmonic very-small-aperture lasers," Appl. Phys. Lett. **91**(2), 021103 (2007).
15. N. Yu, R. Blanchard, J. Fan, T. Edamura, M. Yamanishi, H. Kan, and F. Capasso, "Small divergence edge-emitting semiconductor lasers with two-dimensional plasmonic collimators," Appl. Phys. Lett. **93**(18), 181101 (2008).
16. N. Yu, Q. J. Wang, C. Pflügl, L. Diehl, F. Capasso, T. Edamura, S. Furuta, M. Yamanishi, and H. Kan, "Semiconductor lasers with integrated plasmonic polarizers," Appl. Phys. Lett. **94**(15), 151101 (2009).
17. A. Drezet, C. Genet, and T. W. Ebbesen, "Miniature plasmonic wave plates," Phys. Rev. Lett. **101**(4), 043902 (2008).
18. E. Laux, C. Genet, T. Skauli, and T. W. Ebbesen, "Plasmonic photon sorters for spectral and polarimetric imaging," Nat. Photonics **2**, 161–164 (2008).

19. W. Srituravanich, L. Pan, Y. Wang, C. Sun, D. B. Bogy, and X. Zhang, "Flying plasmonic lens in the near field for high-speed nanolithography," Nat. Nanotechnol. **3**(12), 733–737 (2008).
20. F. I. Baida, D. Van Labeke, and B. Guizal, "Enhanced confined light transmission by single subwavelength apertures in metallic films," Appl. Opt. **42**(34), 6811–6815 (2003).
21. A. Agrawal, H. Cao, and A. Nahata, "Time-domain analysis of enhanced transmission through a single subwavelength aperture," Opt. Express **13**(9), 3535–3542 (2005).
22. M. Beruete, I. Campillo, J. S. Dolado, J. E. Rodriguez-Seco, E. Perea, F. Falcone, and M. Sorolla, ""Very Low-Profile "Bull's Eye" Feeder Antenna," IEEE Antennas Wirel. Propag. Lett. **4**(1), 365–368 (2005).
23. T. Ishi, J. Fujikata, and K. Ohashi, "Large Optical Transmission through a Single Subwavelength Hole Associated with a Sharp-Apex Grating," Jpn. J. Appl. Phys. **44**(4), L170–L172 (2005).
24. C. K. Chang, D. Z. Lin, C. S. Yeh, C. K. Lee, Y. C. Chang, M. W. Lin, J. T. Yeh, and J. M. Liu, "Similarities and differences for light-induced surface plasmons in one- and two-dimensional symmetrical metallic nanostructures," Opt. Lett. **31**(15), 2341–2343 (2006).
25. P. D. Flammer, I. C. Schick, R. T. Collins, and R. E. Hollingsworth, "Interference and resonant cavity effects explain enhanced transmission through subwavelength apertures in thin metal films," Opt. Express **15**(13), 7984–7993 (2007).
26. N. Sedoglavich, J. C. Sharpe, R. Künnemeyer, and S. Rubanov, "Polarisation and wavelength selective transmission through nanohole structures with multiple grating geometry," Opt. Express **16**(8), 5832–5837 (2008).
27. K. L. Shuford, M. A. Ratner, S. K. Gray, and G. C. Schatz, "Finite-difference time-domain studies of light transmission through nanohole structures," Appl. Phys. B **84**(1-2), 11–18 (2006).
28. E. Popov, M. Nevière, A.-L. Fehrembach, and N. Bonod, "Optimization of plasmon excitation at structured apertures," Appl. Opt. **44**(29), 6141–6154 (2005).
29. N. Bonod, E. Popov, D. Gérard, J. Wenger, and H. Rigneault, "Field enhancement in a circular aperture surrounded by a single channel groove," Opt. Express **16**(3), 2276–2287 (2008).
30. O. T. A. Janssen, H. P. Urbach, and G. W. 't Hooft, "Giant optical transmission of a subwavelength slit optimized using the magnetic field phase," Phys. Rev. Lett. **99**(4), 043902 (2007).
31. Y. Cui, and S. He, "A theoretical re-examination of giant transmission of light through a metallic nano-slit surrounded with periodic grooves," Opt. Express **17**(16), 13995–14000 (2009).
32. F. de León-Pérez, G. Brucoli, F. J. García-Vidal, and L. Martín-Moreno, "Theory on the scattering of light and surface plasmon polaritons by arrays of holes and dimples in a metal film," N. J. Phys. **10**(10), 105017 (2008).
33. A. Degiron, H. J. Lezec, N. Yamamoto, and T. W. Ebbesen, "Optical transmission properties of a single subwavelength aperture in a real metal," Opt. Commun. **239**(1-3), 61–66 (2004).
34. F. Przybilla, A. Degiron, C. Genet, T. W. Ebbesen, F. de Léon-Pérez, J. Bravo-Abad, F. J. García-Vidal, and L. Martín-Moreno, "Efficiency and finite size effects in enhanced transmission through subwavelength apertures," Opt. Express **16**(13), 9571–9579 (2008).
35. F. Przybilla, A. Degiron, J.-Y. Laluet, C. Genet, and T. W. Ebbesen, "Optical transmission in perforated noble and transition metal films," J. Opt. A, Pure Appl. Opt. **8**(5), 458–463 (2006).
36. J. A. Sanchez-Gil, "Surface defect scattering of surface plasmon polaritons: Mirrors and light emitters," Appl. Phys. Lett. **73**(24), 3509–3511 (1998).
37. M. Kuttge, F. J. García de Abajo, and A. Polman, "How grooves reflect and confine surfaceplasmon polaritons," Opt. Express **17**(12), 10385–10392 (2009).
38. F. López-Tejeira, F. García-Vidal, and L. Martín-Moreno, F. J. García-Vidal, and L. Martín-Moreno, "Scattering of surface plasmons by one-dimensional periodic nanoindented surfaces," Phys. Rev. B **72**(16), 161405 (2005).
39. F. J. García-Vidal, H. J. Lezec, T. W. Ebbesen, and L. Martín-Moreno, "Multiple paths to enhance optical transmission through a single subwavelength slit," Phys. Rev. Lett. **90**(21), 213901 (2003).

1. Introduction

In the last decades, surface plasmons (SPs) have generated considerable interest because they offer new opportunities in fundamental research and applications in a variety of fields from sensing to opto-electronics [1–4]. Among the possible SP supporting structures, subwavelength apertures in metal films provide much potential for devices as they combine several advantageous features such as high contrast and extraordinary transmission [4]. A variety of aperture structures have been designed and studied and here we are focusing on the so-called bull's eye structure which consists of a sub-wavelength aperture surrounded by periodic concentric rings as shown in Fig. 1(a). The periodic structure at the interface behaves like an antenna which collects and couples the incident light into SPs at a given wavelength λ, resulting in very high fields above the aperture and therefore in high transmission efficiencies under appropriate conditions [4–7]. The transmission normalized to the hole area can even be larger than the intensity per unit area of the incident light. If the output surface around the aperture is also structured it can give rise to beaming with small angular divergence [8–11].
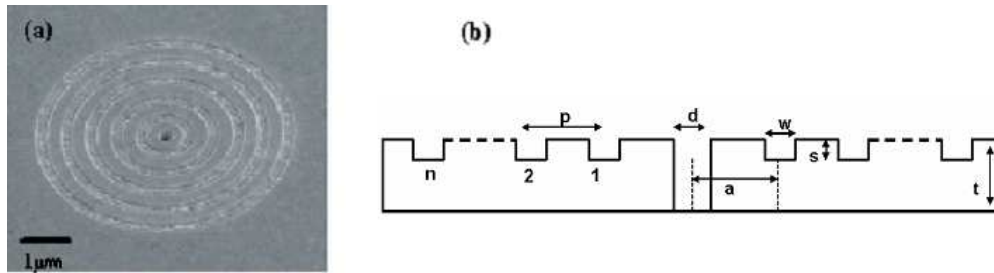
Fig. 1. (a) SEM image of a bull's eye structure. (b) Schematic representation of the structure under study. It consists of a metal film of thickness **t** deposited on a glass substrate. The film is structured by **n** circular grooves of width **w**, depth **s**, separated by a period **p**. A single hole of diameter **d** is milled through the film at a distance **a** from the center of the first groove.

The potential of bull's eyes as device elements has been well recognized. It has already been implemented for instance within photodetector architectures where it improves the signal to noise ratio [12], within VCSEL and QCL lasers [13–16] to control polarization and mode definition, as genuine sub-wavelength optical wave plates [17], for photon sorting [18] and as a subwavelength source in the context of nanolithography [19].

Much work has been performed to understand how such bull's eye structures enhance and focus the transmitted light [9–11,20–31], sometimes using as model a slit flanked by parallel grooves. It is clear that the maximum transmission is obtained when the SP field generated at the metal interface interferes constructively above the aperture. Furthermore the coupling between groove and aperture modes is essential for strengthening the field at the aperture [29]. Experimentally, the dependence of the transmission intensity on parameters such as groove width, hole diameter and depth have been reported [5–8]. In spite of such studies, a systematic exploration of the parameter space defining the optical properties of bull's eyes is still needed as the effect of many geometrical features are interlinked as shown theoretically for slit and groove structures [30]. Here we report the results of such analysis which is especially important when considering the numerous applications just discussed. It allows for the formulation of a simple recipe for preparing regular bull's eye with optimal transmission at a given wavelength in the visible range.

2. Results

Since it is known that the efficiency of the transmission intensity is controlled mainly by the input corrugation and the hole depth (i.e. film thickness) [8,11], we concentrate here on varying all the geometrical parameters on the input surface shown in Fig. 1(b) keeping the hole depth constant. As demonstrated earlier, the transmission intensity is an exponential function of the hole depth in the subwavelength regime [11]. We compare experimental results with theoretical simulations to validate our findings.

For the experimental studies, the structures were milled in a 280 nm thick Au film deposited on a glass substrate using an FEI DB 235 focused ion beam (FIB). Subsequently, the sample was illuminated with collimated white light and the far-field transmission spectra were recorded with an optical microscope Nikon TE200 coupled to an Acton spectrometer and a Princeton instruments CCD camera.

For the theoretical simulations we have made use of the Coupled Mode Method (CMM) formalism [32] for the electromagnetic (EM) field, where the dielectric response of the metal is given by applying surface impedance boundary conditions (SIBC). However, SIBC is only applied at the horizontal surfaces, but not at the vertical walls (inside the cavities), where we consider a perfect metal. To improve this approximation, inside the cavities we consider the propagating constant along the z direction of an infinite annular hole made of real metal. On the other hand, having Perfect Metal inside the cavities let us know analytically the waveguide eigenmodes. In our calculations we consider just the fundamental mode, TE11. To check the validity of our formalism when it is applied to the Bull's eye geometry, we compared FDTD

simulations and ME ones for structures similar to the ones investigated here. In the comparison, the number of annular grooves was reduced to 3 since the actual system (6 grooves) is too large for the FDTD simulation. The good agreement found between the FDTD and CMM results, both in the position with a difference of approximately 25nm, and the relative magnitude of transmission peaks, justify the use of the latter for large systems.

In order to find the optimal transmission intensity the following geometrical parameters were varied: number **n** of grooves, groove width **w**, groove depth **s**, periodicity **p** of the grating, hole diameter **d** and the distance **a** between the first groove and the hole aperture (Fig. 1(b)). The actual values that are explored are confined to those giving rise to transmission resonances in the visible and near IR regions that can be detected by the experimental setup.

2.1. SP resonance and hole diameter
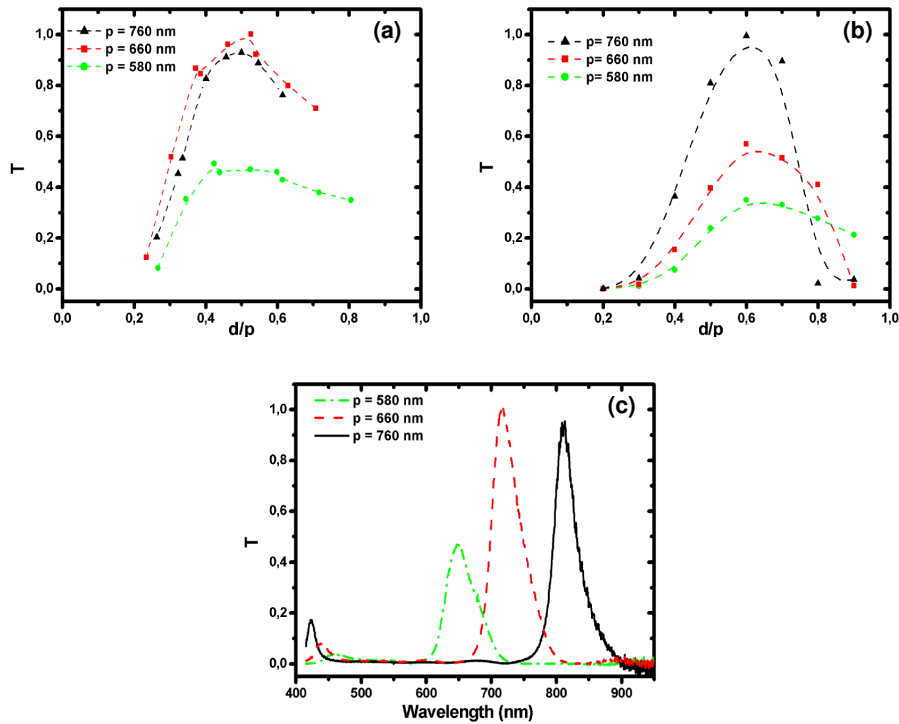
Fig. 2. Effect of the hole diameter on the transmission of a bull's eye (**n** = 7, **s** = 90nm, **w** = 220nm, **t** = 280nm). (a) Relative transmission intensities versus the ratio of hole diameter **d** and groove periodicity **p** for the three series periods (the transmissions have been normalized to the hole area). (b) Theoretical simulations for same systems as in (a). (c) Relative transmission spectra of a bull's eye at three different periods (**p** = 580nm, 660nm, 760nm) **d** = **p**/2.

The Fig. 2(c) shows the transmission spectra for bull's eyes with three different corrugation periods. A strong transmission peak, resulting from the excitation of SPs, is evident around a wavelength slightly larger (ca. 10%) than the period of the structures. This shift is due to the slight increase in the effective index at the interface which in turn defines SP wavelength λ_{SP} roughly equal to the period.

The presence of localized modes [33] in or at the aperture can enhance the transmission but the contribution of such modes to the overall transmission is small compared to that of the SP mode provided by the concentric grooves [5,27]. The difference in the transmission intensities for the 3 different resonance wavelengths in Fig. 2(c) can be explained by a combination of two opposite effects. First, the dielectric constants of the Au in the wavelength

range considered becomes increasingly unfavourable to SPs as the resonance wavelength decreases and approaches the Au interband transition at 550 nm [34]. Secondly as the resonance wavelength increases with **p** for a fixed hole diameter, the aperture will cut the transmission more strongly.

In other words, we expect that the effect of the hole diameter is sensitive to the resonance wavelength since the diameter defines the cutoff wavelength of the aperture. Therefore we have studied the maximum transmission as function of **d/p** for a series of bull's eyes with different period in which we change only the hole diameter and keep the other parameters fixed. In Fig. 2(a) and 2(b) are plotted both the calculated and experimental results and as can be seen the transmission intensity (corrected for hole area) versus **d/p** gives a maximum for **d/p** ~0.5 for all the curves. This can be understood as follows. At diameters smaller than half the period, and therefore half the resonance wavelength, the cutoff function of the hole becomes significant and reduces rapidly the transmission [11]. Beyond the cutoff, the transmission is mainly defined by the area of the aperture as compared to field distribution on the surface. The absolute transmission increases but the intensity normalized to the hole area (as plotted in Fig. 2(a) and 2(b)) decreases because the field is maximum in the center of the structure.

Note that the structures analyzed in Fig. 2 can give rise to transmission intensities normalized to the hole area, greater than 1, in other words, the flux per unit area through the hole is greater than the corresponding incident beam, demonstrating unequivocally the antenna effect of the grooves. When compared to that of a single hole without corrugation, the enhancement at resonance is even greater [35].

2.2. Groove structure
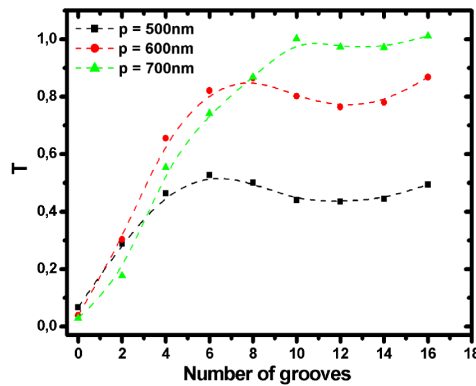
Fig. 3. Relative transmission intensities as a function of the number of grooves for three different periods (**p** = 500nm, 600nm, 700nm with **d** = 250nm, **s** = 90nm, **w** = 220nm, **t** = 280nm).

As mentioned above, the role of the periodic corrugation is to couple the incident light to SPs which concentrate the electromagnetic fields above the aperture leading to very high transmissions. The efficiency of the coupling is directly linked to the geometrical parameters of these grooves. Period p and number of grooves n are two geometrical parameters that directly define the dimension of the structure and play a key role in miniaturization of the active area. Both of these parameters were first varied in order to understand their interdependence and effect on the transmission enhancement. In Fig. 3, the spectral maxima are plotted as a function of **n** for three different values of **p**. As can be seen, the intensity saturates at a given **n** for all three curves. The saturation limit is defined by the SP propagation length in the corrugated surface where it is significantly reduced due to scattering as compared to a flat metal surface [35]. The saturation point and therefore the SP propagation

length is seen to increase with period. This apparent period dependence is mainly due to the fact that the other parameters, such as groove depth, were kept constant as we will see further down.
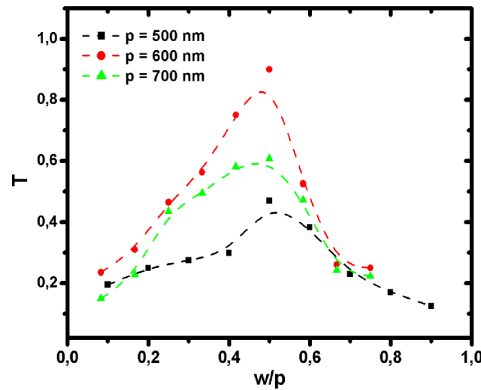
Fig. 4. Relative transmission intensities as a function of the ratio **w/p** for a series of three periods (**p** = 500nm, 600nm and 700nm with **s** = 90nm, **d** = 250nm, **n** = 8).

When considering just the groove width **w**, the maximum transmission intensity has been found for **w** close to half the period (**w/p** ~0.5) [5] which is confirmed in the present study for 3 different periods as can be seen in Fig. 4. This optimal ratio defines a profile which power spectrum is peaked at the SP resonance condition determined by the period. In addition, **w** is interlinked to the groove depth **s** of the corrugations as shown in Fig. 5 where **s** was varied for three different values of **w**, the other parameters being constant. All the curves, both calculated and experimental, show an optimum at the same **s/w** ratio around 0.4, in agreement with theoretical predictions [27]. It indicates a competition of light coupling to SPs and scattering by the grooves versus the damping of the SPs in the grooves [36–38]. The fact that the maximum intensity is found for the s/w curve corresponding to w = 300 nm is probably due to the existence of a mode in the grooves in resonance with the SP mode which has been observed in slit and groove structures [39].
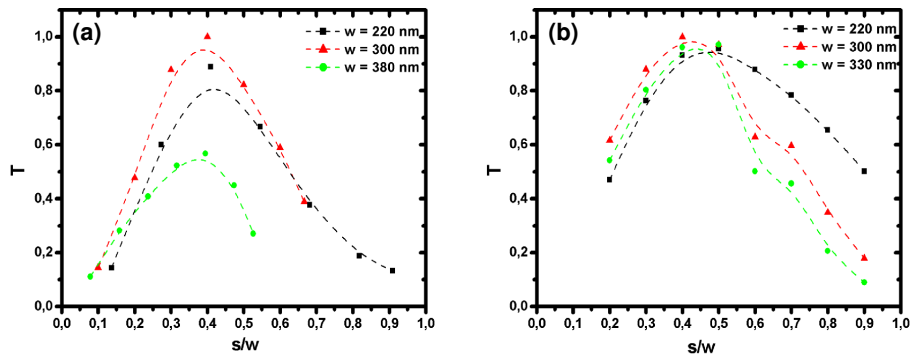
Fig. 5. (a) Effect of shape ratio of the groove **s/w** on the transmission (**a** = 600nm, **d** = 230nm, **p** = 600nm, **n** = 7, **t** = 280nm). (b) Theoretical simulations for the same system than (a).

In order to complete the study of the groove parameters, we investigated separately the relationship between **s** and **w** as a function of **n**. The resulting curves shown in Fig. 6 all exhibit a saturation point. As can be seen in Fig. 6(a), the deeper the groove the earlier the

saturation intensity occurs in agreement with the **s/w** dependence. Note that with **s** = 80nm we obtained a better efficiency because this value is close to the optimal shape ratio (i.e. **s/w** = 0.4). Interestingly the saturation occurs approximately at the same value of **n** for different groove widths (Fig. 6(b)) indicating that in the parameter range studied, **w** does not influence much the SP propagation length. Again the highest intensity is obtained the structure closest to the optimal **s/w**.
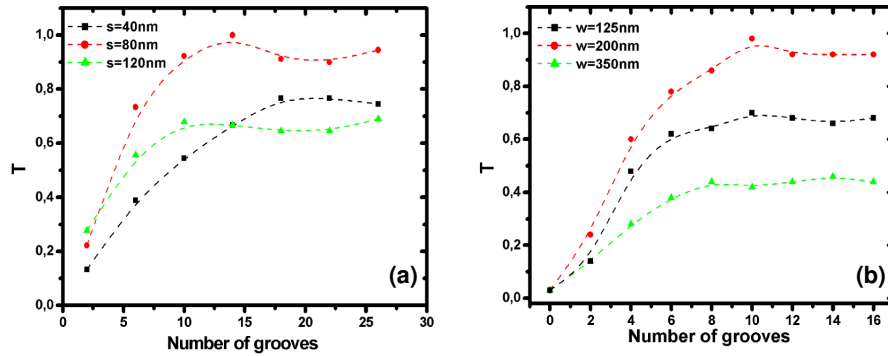
Fig. 6. Effect of the number of corrugations for different values of **s** and **w**. (a) Relative transmission intensities as a function of the number of grooves for a series of three groove depths (**s** = 40nm, 80nm, 120nm with **p** = 600 nm, **w** = 220nm). (b) Relative transmission intensities as a function of the number of grooves for a series of three groove widths (**w** = 125nm, 220nm, 350nm with **p** = 600 nm, **s** = 80nm).

2.3. Distance a

The last parameter that we consider is **a** defined as the distance between the center of aperture to the center of the first groove (see Fig. 1). As can be seen in Fig. 7, the maximum intensity is obtained when **a** is close to the period as might be expected since the aperture is then in phase with the surrounding grating. There is a good agreement between the experimental and the calculated spectra despite a slight shift which we attribute to possible imperfections of the fabricated structures, but also to the approximations done within the CMM formalism regarding the boundary conditions at the groove and the hole walls. Various **a** values have been argued to be optimal [30,31], in particular for slit and groove structures it has been calculated that a maximum transmission intensity is expected at the period, among various possible maxima [31], in agreement with our findings. From a practical point of view, the more important information is that the shape and the position of the resonance changes quite significantly with **a**. It is therefore a parameter that can be used to tweak the resonance once the other features have been optimized.
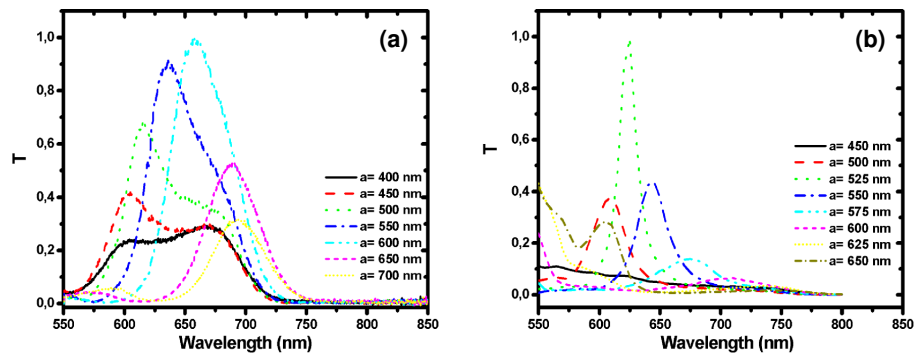
Fig. 7. Effect of distance a on the transmission (**p** = 600nm, **w** = 220nm, **s** = 80nmn, **n** = 6). (a) Experimental data: the distance **a** is varied. (b) Theoretical simulations for the same system than (a).

3. Discussion and conclusions

From the above results it is clear that the geometrical parameters controlling the transmission efficiency of bull's eyes are strongly interlinked. Nevertheless the basic optimization criteria for bull's eye structures can formulated in a straightforward manner. The first item to define is the desired resonance wavelength which in turn determines the period of the structure. The choice of the hole diameter will then be determined whether one would like optimal efficiency as normalized to hole area or highest absolute transmission. For the former, the diameter should be about half the period but for the latter the aperture size can be increased. It should be noted that as the hole size increases relative to the period the spectrum will eventually broaden which is a trade-off. The groove width should also be around half the period with a depth to width ratio at 0.4. The number of grooves should be just enough to reach saturation which is typically around 6 to 10 grooves depending on the geometrical parameters and which reflects the SP propagation length in such optimized structures. This simple optimization recipe should be useful for many applications that can be envisaged for these structures.

Nevertheless other refinements have been conceived that can be useful in certain specific applications. For instance, geometrical features such as sharp ridge and groove profile [23], different hole shapes [20] and non-periodic grooves [28], groove depth gradients [18] or phase shifts for polarisation control [17] have been used or proposed to modify the field distribution and therefore the properties of the bull's eye. There are also questions that remain, notably about the details of the physics at play in these structures which need to be elucidated.

Acknowledgement